DOI: 10.1002/ente.201((will be filled in by the editorial staff))

Ultrathin surface modification by atomic layer deposition on high voltage cathode $LiNi_{0.5}Mn_{1.5}O_4$ for lithium ion batteries

Xin Fang,[b] Mingyuan Ge, [b] Jiepeng Rong, [b] Yuchi Che, [a] Noppadol Aroonyadet, [a] Xiaoli Wang, [a] Yihang Liu,[a] Anyi Zhang, [b] and Chongwu Zhou*[a]

Atomic layer deposition (ALD) has been employed to modify the surface of high voltage cathode $LiNi_{0.5}Mn_{1.5}O_4$ by coating ultrathin Al_2O_3 layer on the electrodes. The ultrathin layer of Al_2O_3 can suppress the undesirable reactions during cycling, while maintaining the electron and ion conductivity of the electrode. The ALD Al_2O_3 coated $LiNi_{0.5}Mn_{1.5}O_4$ showed remarkable improvement over bare $LiNi_{0.5}Mn_{1.5}O_4$. After 200 cycles, the ALD Al_2O_3 coated $LiNi_{0.5}Mn_{1.5}O_4$ showed 91% capacity retention when the bare $LiNi_{0.5}Mn_{1.5}O_4$ can only maintain 75% in the same testing condition. In addition, the ALD coated $LiNi_{0.5}Mn_{1.5}O_4$ maintained 63% capacity retention after as long as 900 cycles. At an elevated temperature of 55 ºC, the ALD Al_2O_3 coated $LiNi_{0.5}Mn_{1.5}O_4$ still delivered 116 mAh/g at the 100th cycle, in comparison, the capacity for bare $LiNi_{0.5}Mn_{1.5}O_4$ decreased to 98 mAh/g. According to the results from charge/discharge test and AC impedance test, the improvement is ascribed to the reduced overpotental and Li ion surface diffusion impedance. The promising results demonstrate the potential of developing high energy and long life lithium ion batteries with highly scalable $LiNi_{0.5}Mn_{1.5}O_4$ preparation and broadly applicable ALD process.

Introduction

Since first commercialized by Sony in the early 1990s, lithium ion batteries have been widely recognized as highly efficient power source and energy storage devices.[1, 2] The energy density of the lithium ion batteries has been significantly enhanced over the last two decades, mainly through optimizing battery materials and engineering design. However, with the rapid development of electric vehicles (EVs), hybrid electric vehicles (HEVs) and plug-in hybrid electric vehicles (PHEVs), higher demand for lithium ion batteries has been raised.[3-5] As the energy density of a lithium ion battery is calculated by the integration of working voltage over the total capacity,[2] increasing the working voltage has emerged as one of the most important methods in increasing the energy density of the batteries.

As the anode materials already work at the potential close to metallic lithium, increasing the total voltage of the battery depends on cathode materials. $LiNi_{0.5}Mn_{1.5}O_4$ was studied when people were developing cation-substituted spinel cathode $LiMn_{2-x}M_xO4$ (M = Ni, Co, Fe, Cu, and Cr), for the purpose of suppressing the Jahn-Teller distortion in $LiMn_2O_4$.[6-8] Amine *et al.* reported $LiNi_{0.5}Mn_{1.5}O_4$ as a 3 V cathode in 1996,[9] and the 4.7 V operating voltage was discovered by Dahn *et al.* in 1997.[10] The origin of the increased voltage was attributed to the increased binding energy of Ni 3d electrons, which was found to be 0.5 eV higher than Mn 3d eg electrons. $LiNi_{0.5}Mn_{1.5}O_4$ has received more attention than other cation-substituted spinel cathodes mainly because of the double operation redox couples, Ni^{2+}/Ni^{3+} and Ni^{3+}/Ni^{4+}, which provide high capacity.[8, 10] While numerous studies have shown the promise lithium ion battery prototypes incorporating the high voltage cathode,[11-13] there is still an important barrier we need to overcome. Since the working potential is at the edge of the electrolyte window Eg,[2] side reactions occur between the high voltage cathode surface and the electrolyte.[14-16] Also, $LiPF_6$ based electrolyte unavoidably contains HF, which will react with LixMOy cathode.[17, 18] The undesirable process compromises the life of the batteries.

Surface modification has been reported to be an effective method to suppress the side reactions and enhance the battery performance.[14, 19-23] Various materials have been explored as coating layers to stabilize the surface, such as Al_2O_3,[24, 25] Bi_2O_3,[24, 25] BiOF,[20] ZnO,[14] SiO_2,[26] ZrO_2,[21] Li_3PO_4,[27] $AlPO_4$,[24] ZrP_2O_7,[21] AlF_3,[19] Au,[28] Ag,[29] polyimide,[22] conductive carbon,[23] graphene oxide[30] and so on. Among those coating materials studied previously, although all of them can prevent the surface of $LiNi_{0.5}Mn_{1.5}O_4$ from being directly exposed to electrolyte, metal oxides are believed to act as HF scavenger at the same time[31] thus being ideal in improving the battery performance, especially at elevated temperature. As $LiPF_6$ based electrolyte has become one of the most widely used electrolyte systems, it is beneficial to have a protection layer against the unavoidable HF. However, traditional coating strategy are usually based on solution chemistry,[14, 19, 21, 22, 24] which cannot control the uniformity, conformity and thickness precisely. While using more coating precursors can improve the coverage over the surface of bare $LiNi_{0.5}Mn_{1.5}O_4$, it is difficult to avoid the coating materials forming agglomerated particles. As many metal oxide materials do not have good conductivity, especially Al_2O_3, agglomeration or increased thickness becomes detrimental to the conductivity of the electrode. Certain metal oxide coating, such as Bi_2O_3,[24] has been reported to provide good conductivity, yet this is because Bi_2O_3 experienced structure change and converted to Bi metal during cycling, thus the coating stability is sacrificed. Moreover, for all the metal oxide coatings mentioned above, no

[a] *Y. Che, N. Aroonyadet, X. Wang, Y. Liu, Prof. C. Zhou*
Ming Hsieh Department of Electrical Engineering
University of Southern California
3710 McClintock Ave. Los Angeles, CA 90089, USA
E-mail: chongwuz@usc.edu
[b] *X. Fang, M. Ge, J. Rong, A. Zhang*
Mork Family Department of Chemical Engineering and Mateirals Science
University of Southern California
3710 McClintock Ave. Los Angeles, CA 90089, USA

long cycling performance was reported, in spite of the fact that cycle life is an important criterion in judging the battery performance.

Recently, atomic layer deposition (ALD) has emerged as an advanced technology to improve the performance of lithium ion batteries.[32-49] For example, ALD coating has been reported for materials such as $LiCoO_2$,[41, 42] graphite,[33] and $LiMn_2O_4$.[46-49] However, to the best of our knowledge, there has been no report on employing ALD in surface modification of $LiNi_{0.5}Mn_{1.5}O_4$. In this study, we report the first ultrathin Al_2O_3 coating using ALD for $LiNi_{0.5}Mn_{1.5}O_4$, and we have achieved much improved performance in both room temperature and elevated temperature (55 ℃) cycling test. By coating $LiNi_{0.5}Mn_{1.5}O_4$ with ALD Al_2O_3, the following benefits can be obtained: 1) the coating thickness can be precisely controlled to the scale of Å, which not only minimized the extra mass added to the electrode, but also preserved the conductivity of the electrode, since electrons can tunnel through Al_2O_3 when it is below 4 nm;[50] 2) ALD provides superior coating quality in terms of uniformity and conformity, in contrast, traditional solution chemistry method easily leads to agglomerated Al_2O_3 particles on the surface;[51] 3) ALD can be applied to pre-fabricated electrodes, where all surface that may be exposed to the electrolyte can be covered, but the electron and Li ion path between $LiNi_{0.5}Mn_{1.5}O_4$, carbon black and current collector is not blocked; 4) ALD needs very little precursor and no solvent, thus no waste water is involved. With the above-mentioned advantages of ALD, remarkable improvement of the battery performance was achieved. After 900 cycles, the ALD Al_2O_3 coated $LiNi_{0.5}Mn_{1.5}O_4$ showed 63% capacity retention when the bare $LiNi_{0.5}Mn_{1.5}O_4$ can only maintain 75% after 200 cycles. At an elevated temperature of 55 ℃, the ALD Al_2O_3 coated $LiNi_{0.5}Mn_{1.5}O_4$ delivered 116 mAh/g at the 100th cycle, in comparison, the capacity for bare $LiNi_{0.5}Mn_{1.5}O_4$ decreased to 98 mAh/g. This promising result demonstrated the potential of employing ALD Al_2O_3 coated $LiNi_{0.5}Mn_{1.5}O_4$ for high energy and long life lithium ion batteries.

.

Scheme 1. Schematic diagram showing ALD Al_2O_3 coating on pre-fabricated electrodes.

Results and Discussion

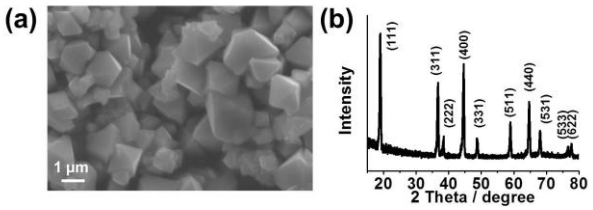

Figure 1. Characterization of as-synthesized $LiNi_{0.5}Mn_{1.5}O_4$ particles. (a) SEM image of as-synthesized $LiNi_{0.5}Mn_{1.5}O_4$ particles. (b) XRD pattern of the as-synthesized $LiNi_{0.5}Mn_{1.5}O_4$ particles.

A variety of preparation methods have been reported to synthesize $LiNi_{0.5}Mn_{1.5}O_4$, including solid state reaction,[52, 53] co-precipitation,[54, 55] sol-gel method,[56, 57] polymer assisted synthesis,[58-60] molten salt method,[61] hydrothermal method[62] and so on. Among the above mentioned methods, solid state reaction and co-precipitation are most mature and scalable in industrial application. Here we adopted solid state reaction since it does not involve any waste solvent and therefore is more environmentally benign than other methods. Figure 1a shows the scanning electron microscopy (SEM) image of the as-synthesized $LiNi_{0.5}Mn_{1.5}O_4$ particles. The size of the particles is mostly around 1 μm and the shape is polyhedral. Figure 1b presents the X-ray diffraction (XRD) pattern of the as-synthesized $LiNi_{0.5}Mn_{1.5}O_4$ particles. The peaks correspond to the typical cubic structure of spinel $LiNi_{0.5}Mn_{1.5}O_4$, which agrees with literature.[63]

According to previous studies,[64] $LiNi_{0.5}Mn_{1.5}O_4$ has two space groups: $Fd\bar{3}m$ and $P4_332$. In both of these two phases, oxygen atoms form a cubic close packing, Mn and Ni atoms occupy half of the octahedral sites and Li atoms occupy one eighth of the tetrahedral sites. In the octahedral sites, Mn and Ni may be orderly or disorderly arranged which correspond to $P4_332$ and $Fd\bar{3}m$, respectively. It is difficult to distinguish the two phases from XRD pattern, but we can see the existence of $Fd\bar{3}m$ spinel from our charge/discharge curves, where clearly show the small Mn^{3+} plateau at around 4.1 V, a fingerprint of $Fd\bar{3}m$ $LiNi_{0.5}Mn_{1.5}O_4$. We note that there are some oxygen vacancies in the $Fd\bar{3}m$ spinel, so the actual chemical formula should be $LiNi_{0.5}Mn_{1.5}O_{4-\delta}$, although $LiNi_{0.5}Mn_{1.5}O_4$ is commonly used in this paper and literature. It has been reported that $Fd\bar{3}m$ spinel has better performance than $P4_332$ spinel.[64] However, Mn^{3+} ions are inclined to decompose into Mn^{2+} and Mn^{4+}, the former of which is easy to dissolve into the electrolyte.[65] It is also reported that Ni^{2+} has the tendency to dissolve as well.[54, 65] In this regard, a coating layer is highly desirable to protect the metal ions from dissolution thus improving the performance of the batteries.

ALD was performed on pre-fabricated electrodes made from $LiNi_{0.5}Mn_{1.5}O_4$, as shown in Scheme 1. We note that the thickness of the Al_2O_3 layer should be much smaller than that of the electrode. To make the Al_2O_3 layer visible, the schematic is not drawn to scale. After coating the electrode with Al_2O_3, energy dispersive X-ray spectroscopy (EDX) was used to confirm the successful coating by checking the existence of Al on the electrode. Figure 2a shows the mapping of the surface from the top of the electrode (mapping area is shown on the upper left). From the distribution of Al we can confirm the uniformity and conformity of the deposited Al_2O_3 layer. We believe it is because

$LiNi_{0.5}Mn_{1.5}O_4$ possesses hydroxyl-terminated surface, which is common for metal oxides, and this surface feature is favored in ALD process.[33] This way ALD can be directly conducted on $LiNi_{0.5}Mn_{1.5}O_4$ electrodes without any pre-treatment. Figure 2b displays the EDX mapping result on a cross-section of the $LiNi_{0.5}Mn_{1.5}O_4$ electrode (mapping area is shown on the upper left). We intentionally avoided including the most bottom part of the electrode to eliminate the inadvertent Al signal from the current collector. The distribution of Al shows that the ALD precursors can diffuse through the pores of the pre-fabricated electrodes, hence the surface of the pores inside the electrode can also be covered. This phenomenon is in agreement with what has been shown with ALD Al_2O_3 coated natural graphite, where the ALD precursors deposited a conformal Al_2O_3 film in the torturous path of the entire electrode structure.[33] We believe this is favorable in protecting the electrode from the undesired reactions, since any surface area that would be in contact with the electrolyte can be covered in the ALD process. To show the morphology of ALD Al_2O_3 coating on $LiNi_{0.5}Mn_{1.5}O_4$, high-resolution TEM images are presented in Figure 2c and 2d. The images clearly show the Al_2O_3 layer on the outer surface of $LiNi_{0.5}Mn_{1.5}O_4$ (Figure 2c) and the crystalline nature of the $LiNi_{0.5}Mn_{1.5}O_4$ particles (Figure 2d). In Figure 2c, the Al_2O_3 layer comes from 30 cycles ALD coating. The thickness of 3-4 nm Al_2O_3 corresponds well with the growth rate of 0.12 nm per ALD cycle reported in literature.[41]

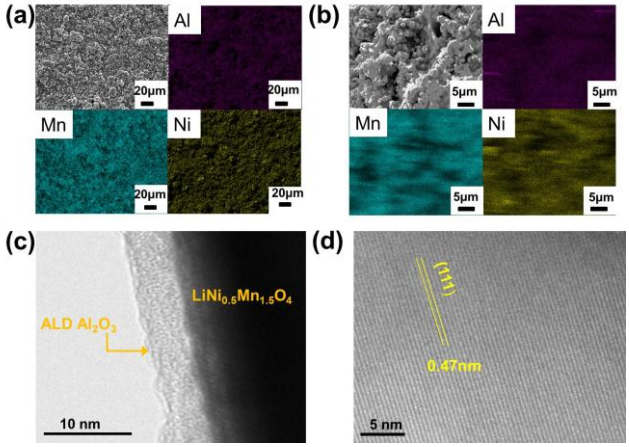

Figure 2. EDX elemental mapping of ALD Al_2O_3 coated $LiNi_{0.5}Mn_{1.5}O_4$ electrode (a) from the top and (b) from a cross-section. The mapping area is shown on the upper left. High-resolution TEM images showing (c) morphology of 30 cycles ALD Al_2O_3 coated on $LiNi_{0.5}Mn_{1.5}O_4$ and (d) the crystalline nature of $LiNi_{0.5}Mn_{1.5}O_4$ particles.

To evaluate the effect of ALD Al_2O_3 coating on the electrochemical performance, 2032 coin cells were assembled with metallic lithium as counter electrodes. The uncoated $LiNi_{0.5}Mn_{1.5}O_4$ electrodes were also tested at the same condition as a comparison. According to literature,[33, 41, 42, 44, 45] once the coating thickness exceeds a threshold value, the electrochemical stability will be affected by the kinetics associated with ion and electron transportation. The maximum allowed thickness can be different for different materials. We have also studied the effect of thickness of oxide coating. With our home-made ALD system, 3, 10 and 30 cycles of ALD Al_2O_3 were coated on the electrodes and the battery performance is shown in Figure S1. It is clear that 3and 10 cycles ALD coating showed better performance than 30 cycles at room temperature (shown in Figure S1a and S1b). Further test at elevated temperature (55 ℃) of 3 and 10 cycles ALD coating demonstrated that 10 cycles ALD coating should be the optimized thickness in our system, since 3 cycles ALD coating cannot greatly enhance the high temperature performance (shown in Figure S1c). In this regard, 10 cycles ALD was chosen as a representative for the analysis of ALD coated $LiNi_{0.5}Mn_{1.5}O_4$ in comparison with bare $LiNi_{0.5}Mn_{1.5}O_4$.

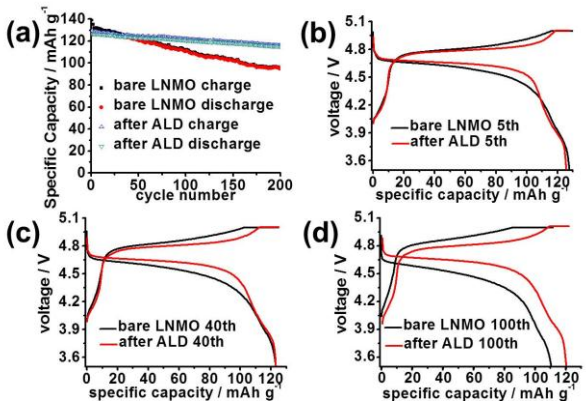

Figure 3. Room temperature cycling test results. (a) Comparison of cyclability of ALD Al_2O_3 coated and bare $LiNi_{0.5}Mn_{1.5}O_4$ at current rate of C/2 (1C = 140 mA g^{-1}). Charge/discharge curves of the (b) 5th,(c) 40th and (d) 100th cycle from both ALD Al_2O_3 coated and bare $LiNi_{0.5}Mn_{1.5}O_4$.

Figure 3a shows the results from cycling test of the $LiNi_{0.5}Mn_{1.5}O_4$ cathode with and without Al_2O_3 ALD. It is evident that the batteries showed better capacity retention after Al_2O_3 coating. After 200 cycles at the charging/discharging rate of C/2 (1C = 140 mA g^{-1}), ALD Al_2O_3 coated $LiNi_{0.5}Mn_{1.5}O_4$ cathode maintained 91% of the original capacity. In comparison, the bare $LiNi_{0.5}Mn_{1.5}O_4$ cathode can only deliver 75% of the original capacity at the 200th cycle. Although the batteries showed very small difference in capacity retention in the first 40 cycles, the improvement from ALD coating became much more obvious with the extending cycling test. We believe this is because the thin layer of Al_2O_3 can help to form stable solid electrolyte interface (SEI) and protect the cathode material from undesirable side reactions, such as HF etching and metal ions dissolution. It has been reported that HF, generated by trace amount of moisture reacting with $LiPF_6$ based electrolyte, continuously attacks the electrode active material and causes capacity fading as cycling goes by.[51] This effect is not observed during the early stage of cycling, but gradually turns obvious in extensively cycled batteries. Figure 3b, 3c and 3d represent the charge/discharge curves of the 5th, 40th and 100th cycle, respectively. It is evident that the overpotential of the batteries with bare $LiNi_{0.5}Mn_{1.5}O_4$ increased significantly compared with that of the ALD Al_2O_3 coated batteries. Also, the decrease of capacity is more obvious in bare $LiNi_{0.5}Mn_{1.5}O_4$ batteries. This phenomenon clearly shows the influence of the side reactions from electrolyte. As more

byproducts adhere to the surface of the electrode and separator, the resistance increases with cycling thus leading to the increase of overpotential. In addition, Mn and Ni ions have been found to dissolve into the electrolyte and get reduced and deposited on the surface of the anode.[54, 65] As neither Mn nor Ni metal is good lithium ion conductor, this dissolution of metal ions not only causes loss of capacity, but also increases the total resistance of the batteries. In comparison, the ALD Al_2O_3 coated $LiNi_{0.5}Mn_{1.5}O_4$ shows smaller overpotantial and better capacity retention, which clearly demonstrates the merits from the thin protection layer of Al_2O_3.

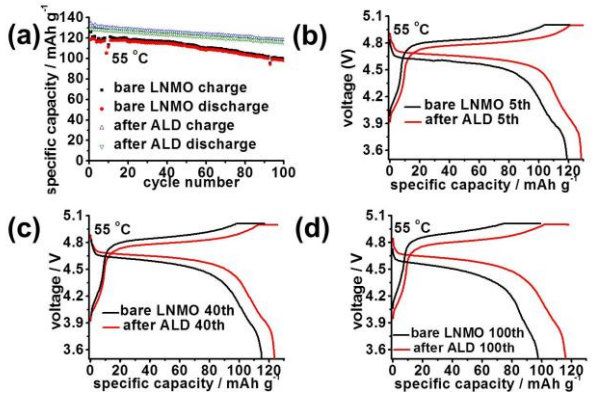

Figure 4. 55 ºC cycling test results. (a) Comparison of cyclability of ALD Al_2O_3 coated and bare $LiNi_{0.5}Mn_{1.5}O_4$ at current rate of C/2 (1C = 140 mA g^{-1}). Charge/discharge curves of the (b) 5th,(c) 40th and (d) 100th cycle from both ALD Al_2O_3 coated and bare $LiNi_{0.5}Mn_{1.5}O_4$.

To further assess the improvement from ALD Al_2O_3 coating, the batteries were also tested at an aggressive temperature of 55 ℃, since lithium ion batteries need to operate at a wide temperature range in practical applications. Figure 4a shows the results from high temperature cycling test. At 55 ℃, the ALD coated $LiNi_{0.5}Mn_{1.5}O_4$ performs favorably over the bare $LiNi_{0.5}Mn_{1.5}O_4$ in terms of both capacity and stability. After cycling at 55 ℃ for 100 cycles, the ALD Al_2O_3 coated $LiNi_{0.5}Mn_{1.5}O_4$ delivered 116 mAh/g, corresponding to 90% of the original capacity, but the bare $LiNi_{0.5}Mn_{1.5}O_4$ can only maintain 98 mAh/g, which is less than 83% of the initial capacity. The charge/discharge curves of the 5th, 40th and 100th cycle at 55 ℃ are shown in Figure 4b, 4c and 4d, respectively. The difference in overpotential and capacity retention between the Al_2O_3 ALD coated $LiNi_{0.5}Mn_{1.5}O_4$ and bare $LiNi_{0.5}Mn_{1.5}O_4$ became increasingly evident with the cycling test going on. Since the side reactions from electrolyte became more pronounced at elevated temperature,[22] the degradation of the bare $LiNi_{0.5}Mn_{1.5}O_4$ became more severe if comparing Figure 3d and 4d. In contrast, the ALD Al_2O_3 coated $LiNi_{0.5}Mn_{1.5}O_4$ exhibited better performance in suppressing the undesirable effects. The results from high temperature test further demonstrated the advantage of having the ALD Al_2O_3 surface protection layer on $LiNi_{0.5}Mn_{1.5}O_4$ electrodes.

The promising results from ALD coated $LiNi_{0.5}Mn_{1.5}O_4$ can be ascribed to the following reasons. First, Al_2O_3 can act as HF scavenger hence $LiNi_{0.5}Mn_{1.5}O_4$ is protected from HF etching. As reported in Al_2O_3 coated layered lithium transition metal oxide cathode,[51] the amount of HF generated during cycling is quite suppressed by Al_2O_3. This way the active cathode material is protected, especially at elevated temperature. Second, the Al_2O_3 layer prevented $LiNi_{0.5}Mn_{1.5}O_4$ from being directly exposed to electrolyte, hence the dissolution of metal ions was suppressed. As both Mn and Ni ions have been reported to dissolve into the electrolyte, which lead to an increase of impedance, it is beneficial to cut off the direct exposure with the Al_2O_3 layer. In addition, due to the advantage of ALD, the coating layer can cover any surface that may be exposed to electrolyte uniformly as mentioned before, however, the connection between $LiNi_{0.5}Mn_{1.5}O_4$ other electrode materials, such as carbon black and PVDF, is not blocked. Electrons and Li ions can travel from $LiNi_{0.5}Mn_{1.5}O_4$ to carbon black or Al current collector without any added resistance. Another advantage of ALD is that it has atomic thickness control, which cannot be achieved with traditional solution chemistry. Usually the overall specific capacity is lowered as the coating layer is an extra weight added to the electrodes,[51] but negligible weight is added in the ultrathin coating *via* ALD. ALD process also eliminates the possibility that Al_2O_3 forms agglomerated particles on the surface of the cathode, which is shown with solution chemistry coating.[51] Since electrons can tunnel through the Al_2O_3 layer when it is less than 4 nm,[50] the precise control of thickness plays an important role in preserving the conductivity of the electrodes with negligible extra weight.

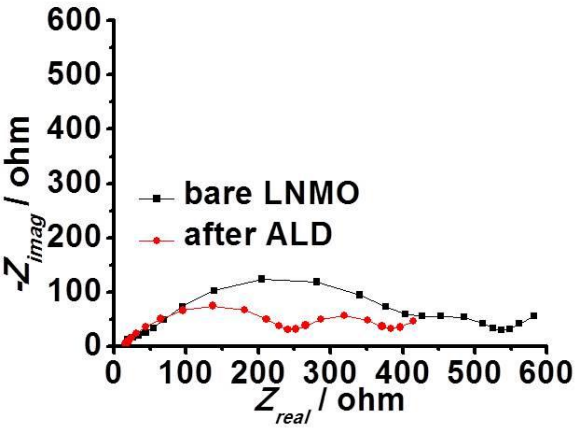

Figure 5. AC impedance test results of both ALD Al_2O_3 coated and bare $LiNi_{0.5}Mn_{1.5}O_4$ after cycling at 55 ºC for 100 cycles.

To confirm our analysis, electrochemical impedance spectra (EIS) of both bare $LiNi_{0.5}Mn_{1.5}O_4$ and ALD coated $LiNi_{0.5}Mn_{1.5}O_4$ were collected after 100 cycles at 55 ℃. According to literature,[15] the first semicircle (at high frequency) represents the Li ion diffusion through the surface layer and the second semicircle (at medium to low frequency) represents charge transfer reaction. The bare $LiNi_{0.5}Mn_{1.5}O_4$ showed much larger impedance in the first semicircle, meaning the Li ions encountered larger barrier when diffuse through surface layer of bare $LiNi_{0.5}Mn_{1.5}O_4$. This is an indication that the ultrathin Al_2O_3 layer can suppress the undesirable reactions during cycling, hence

the surface of the electrode was protected and the increase in surface impedance was also suppressed. In addition, the similar charge transfer resistance between bare and ALD coated $LiNi_{0.5}Mn_{1.5}O_4$ supports our analysis that this ultrathin Al_2O_3 layer did not hinder the electron transfer obviously.

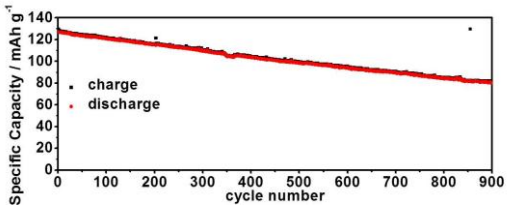

Figure 6. Long cycling performance of ALD Al_2O_3 coated $LiNi_{0.5}Mn_{1.5}O_4$ at C/2.

With all the benefits brought by ALD Al_2O_3 coating mentioned previously, the batteries showed superior long cycling performance. As shown in Figure 6, 63% capacity retention was achieved after 900 cycles, which converts to only 0.04% capacity decay per cycle. The remarkable cycling performance demonstrated the stability and effectiveness of surface modification from ALD Al_2O_3 coating, and also the potential of employing this strategy in the application of high energy and long life lithium ion batteries.

Conclusion

In summary, we have successfully synthesized $LiNi_{0.5}Mn_{1.5}O_4$ with highly scalable solid state reaction and coated ultrathin Al_2O_3 layer *via* ALD on the electrodes. With the advantage of uniformity, conformity and thickness control from ALD, the active material $LiNi_{0.5}Mn_{1.5}O_4$ is protected from direct exposure to the liquid electrolyte and the conductivity is reserved. The batteries with ALD Al_2O_3 coating showed much improved performance over bare $LiNi_{0.5}Mn_{1.5}O_4$. The capacity retention after ALD coating is 63% after 900 cycles. In comparison, the bare $LiNi_{0.5}Mn_{1.5}O_4$ can only maintain 75% of the original capacity after 200 cycles. At elevated temperature of 55 ℃, the ALD coated $LiNi_{0.5}Mn_{1.5}O_4$ showed 91% capacity retention after 100 cycles while the bare $LiNi_{0.5}Mn_{1.5}O_4$ showed less than 83%. Analysis of overpotential and impedance confirmed that the improvement was brought by reducing undesirable reactions during cycling, thus suppressing the increase in the barrier of Li ion and electron transportation. The strategy of coating ultrathin Al_2O_3 *via* ALD on high voltage cathode $LiNi_{0.5}Mn_{1.5}O_4$ leads to new opportunities in developing high energy density lithium ion batteries, and the promising performance demonstrates the potential of employing the surface modified high voltage cathode in the application of portable electronics, EVs, HEVs and PHEVs in the future.

Experimental Section

Material synthesis

$LiNi_{0.5}Mn_{1.5}O_4$ particles were synthesized *via* solid state reactions. Nickel acetate ($Ni(Ac)_2•4H_2O$) and manganese acetate ($Mn(Ac)_2•4H_2O$) were mixed at a molar ratio of Ni : Mn = 1 : 3 and milled in a mortar. After heating at 500 ℃ for 5 hours, lithium acetate ($LiAc•2H_2O$) was added to the mixture with a molar ratio of Li : Ni : Mn = 2.1 : 1 : 3 (5% excess Li source was added in order to make up for the volatilization of Li during calcination), and the mixture was heated to 500 ℃ for 5 hours once more. Then the mixture was milled and sintered at 950 ℃ for 10 hours followed by annealing at 700 ℃ for 10 hours.

ALD process

ALD was performed on pre-fabricated electrode with a home-made system. The electrodes were prepared with traditional slurry casting method on Al current collector. The weight ratio in the electrode was active material : poly(vinylidene fluoride) : carbon black = 8 : 1 : 1. Trimethylaluminum (TMA) and H_2O were used as precursors. ALD were performed at the temperature of 90 ℃ and pressure of $6x10^{-1}$ torr in a vacuum chamber.

Electrochemical measurements

CR 2032 coin cells were assembled with Li metal as counter electrodes. 1.2 M solution of $LiPF_6$ in ethylene carbonate (EC) and dimethyl carbonate (DMC) (3:7) was used as electrolyte. The batteries were cycled in the voltage range of 3.5 V ~ 5 V at both room temperature and elevated temperature of 55 ℃. Electrochemical impedance spectra (EIS) were collected with AC voltage at 5 mV amplitude and frequency range of 100 kHz to 10 mHz. The batteries were fully charged and then rested to reach equilibrium before the impedance test.

Keywords: atomic layer deposition • lithium ion batteries • high voltage cathode • $LiNi_{0.5}Mn_{1.5}O_4$ • ultrathin Al_2O_3 coating

[1] M. Armand, J. M. Tarascon, *Nature* **2008**, *451*, 652-657.
[2] J. B. Goodenough, Y. Kim, *J Power Sources* **2011**, *196*, 6688-6694.
[3] J. M. Tarascon, M. Armand, *Nature* **2001**, *414*, 359-367.
[4] N. S. Choi, Z. H. Chen, S. A. Freunberger, X. L. Ji, Y. K. Sun, K. Amine, G. Yushin, L. F. Nazar, J. Cho, P. G. Bruce, *Angew Chem Int Edit* **2012**, *51*, 9994-10024.
[5] T. H. Kim, J. S. Park, S. K. Chang, S. Choi, J. H. Ryu, H. K. Song, *Adv Energy Mater* **2012**, *2*, 860-872.
[6] J. M. Tarascon, E. Wang, F. K. Shokoohi, W. R. Mckinnon, S. Colson, *J Electrochem Soc* **1991**, *138*, 2859-2864.
[7] R. J. Gummow, A. Dekock, M. M. Thackeray, *Solid State Ionics* **1994**, *69*, 59-67.
[8] K. Amine, H. Tukamoto, H. Yasuda, Y. Fujita, *J Power Sources* **1997**, *68*, 604-608.
[9] K. Amine, H. Tukamoto, H. Yasuda, Y. Fujita, *J Electrochem Soc* **1996**, *143*, 1607-1613.
[10] Q. M. Zhong, A. Bonakdarpour, M. J. Zhang, Y. Gao, J. R. Dahn, *J Electrochem Soc* **1997**, *144*, 205-213.
[11] H. G. Jung, M. W. Jang, J. Hassoun, Y. K. Sun, B. Scrosati, *Nat Commun* **2011**, *2*.
[12] J. Hassoun, S. Panero, P. Reale, B. Scrosati, *Adv Mater* **2009**, *21*, 4807-4810.
[13] H. F. Xiang, X. Zhang, Q. Y. Jin, C. P. Zhang, C. H. Chen, X. W. Ge, *J Power Sources* **2008**, *183*, 355-360.
[14] Y. K. Sun, Y. S. Lee, M. Yoshio, K. Amine, *Electrochem Solid St* **2002**, *5*, A99-A102.
[15] R. Alcantara, M. Jaraba, P. Lavela, J. L. Tirado, *J Electroanal Chem* **2004**, *566*, 187-192.
[16] H. Duncan, Y. Abu-Lebdeh, I. J. Davidson, *J Electrochem Soc* **2010**, *157*, A528-A535.

[17] H. Sclar, D. Kovacheva, E. Zhecheva, R. Stoyanova, R. Lavi, G. Kimmel, J. Grinblat, O. Girshevitz, F. Amalraj, O. Haik, E. Zinigrad, B. Markovsky, D. Aurbach, *J Electrochem Soc* **2009**, *156*, A938-A948.
[18] B. Markovsky, D. Kovacheva, Y. Talyosef, M. Gorova, J. Grinblat, D. Aurbach, *Electrochem Solid St* **2006**, *9*, A449-A453.
[19] J. G. Li, Y. Y. Zhang, J. J. Li, L. Wang, X. M. He, J. Gao, *Ionics* **2011**, *17*, 671-675.
[20] H. B. Kang, S. T. Myung, K. Amine, S. M. Lee, Y. K. Sun, *J Power Sources* **2010**, *195*, 2023-2028.
[21] H. M. Wu, I. Belharouak, A. Abouimrane, Y. K. Sun, K. Amine, *J Power Sources* **2010**, *195*, 2909-2913.
[22] J. H. Cho, J. H. Park, M. H. Lee, H. K. Song, S. Y. Lee, *Energ Environ Sci* **2012**, *5*, 7124-7131.
[23] T. Y. Yang, N. Q. Zhang, Y. Lang, K. N. Sun, *Electrochim Acta* **2011**, *56*, 4058-4064.
[24] J. Liu, A. Manthiram, *Chem Mater* **2009**, *21*, 1695-1707.
[25] J. Liu, A. Manthiram, *J Electrochem Soc* **2009**, *156*, S13-S13.
[26] Y. K. Fan, J. M. Wang, Z. Tang, W. C. He, J. Q. Zhang, *Electrochim Acta* **2007**, *52*, 3870-3875.
[27] Y. Kobayashi, H. Miyashiro, K. Takei, H. Shigemura, M. Tabuchi, H. Kageyama, T. Iwahori, *J Electrochem Soc* **2003**, *150*, A1577-A1582.
[28] J. Arrebola, A. Caballero, L. Hernan, J. Morales, E. R. Castellon, J. R. R. Barrado, *J Electrochem Soc* **2007**, *154*, A178-A184.
[29] J. Arrebola, A. Caballero, L. Hernan, J. Morales, E. R. Castellon, *Electrochem Solid St* **2005**, *8*, A303-A307.
[30] X. Fang, M. Y. Ge, J. P. Rong, C. W. Zhou, *Journal of Materials Chemistry A* **2013**, *1*, 4083-4088.
[31] Z. H. Chen, Y. Qin, K. Amine, Y. K. Sun, *J Mater Chem* **2010**, *20*, 7606-7612.
[32] X. B. Meng, X. Q. Yang, X. L. Sun, *Adv Mater* **2012**, *24*, 3589-3615.
[33] Y. S. Jung, A. S. Cavanagh, L. A. Riley, S. H. Kang, A. C. Dillon, M. D. Groner, S. M. George, S. H. Lee, *Adv Mater* **2010**, *22*, 2172-+.
[34] I. Lahiri, S. M. Oh, J. Y. Hwang, C. Kang, M. Choi, H. Jeon, R. Banerjee, Y. K. Sun, W. Choi, *J Mater Chem* **2011**, *21*, 13621-13626.
[35] L. A. Riley, A. S. Cavanagh, S. M. George, Y. S. Jung, Y. F. Yan, S. H. Lee, A. C. Dillon, *Chemphyschem* **2010**, *11*, 2124-2130.
[36] L. A. Riley, A. S. Cavanagh, S. M. George, S. H. Lee, A. C. Dillon, *Electrochem Solid St* **2011**, *14*, A29-A31.
[37] E. Kang, Y. S. Jung, A. S. Cavanagh, G. H. Kim, S. M. George, A. C. Dillon, J. K. Kim, J. Lee, *Adv Funct Mater* **2011**, *21*, 2430-2438.
[38] X. C. Xiao, P. Lu, D. Ahn, *Adv Mater* **2011**, *23*, 3911-+.
[39] Y. He, X. Q. Yu, Y. H. Wang, H. Li, X. J. Huang, *Adv Mater* **2011**, *23*, 4938-4941.
[40] D. Ahn, X. C. Xiao, *Electrochem Commun* **2011**, *13*, 796-799.
[41] Y. S. Jung, A. S. Cavanagh, A. C. Dillon, M. D. Groner, S. M. George, S. H. Lee, *J Electrochem Soc* **2010**, *157*, A75-A81.
[42] I. D. Scott, Y. S. Jung, A. S. Cavanagh, Y. F. An, A. C. Dillon, S. M. George, S. H. Lee, *Nano Lett* **2011**, *11*, 414-418.
[43] H. M. Cheng, F. M. Wang, J. P. Chu, R. Santhanam, J. Rick, S. C. Lo, *J Phys Chem C* **2012**, *116*, 7629-7637.
[44] L. A. Riley, S. Van Ana, A. S. Cavanagh, Y. F. Yan, S. M. George, P. Liu, A. C. Dillon, S. H. Lee, *J Power Sources* **2011**, *196*, 3317-3324.
[45] Y. S. Jung, A. S. Cavanagh, Y. F. Yan, S. M. George, A. Manthiram, *J Electrochem Soc* **2011**, *158*, A1298-A1302.
[46] D. S. Guan, J. A. Jeevarajan, Y. Wang, *Nanoscale* **2011**, *3*, 1465-1469.
[47] J. Q. Zhao, Y. Wang, *J Solid State Electr* **2013**, *17*, 1049-1058.
[48] D. S. Guan, Y. Wang, *Ionics* **2013**, *19*, 1-8.
[49] X. N. Luan, D. S. Guan, Y. Wang, *J Nanosci Nanotechno* **2012**, *12*, 7113-7120.
[50] M. D. Groner, J. W. Elam, F. H. Fabreguette, S. M. George, *Thin Solid Films* **2002**, *413*, 186-197.
[51] S. T. Myung, K. Izumi, S. Komaba, Y. K. Sun, H. Yashiro, N. Kumagai, *Chem Mater* **2005**, *17*, 3695-3704.
[52] X. Y. Feng, C. Shen, X. Fang, C. H. Chen, *J Alloy Compd* **2011**, *509*, 3623-3626.
[53] X. Fang, Y. Lu, N. Ding, X. Y. Feng, C. Liu, C. H. Chen, *Electrochim Acta* **2010**, *55*, 832-837.
[54] X. Fang, N. Ding, X. Y. Feng, Y. Lu, C. H. Chen, *Electrochim Acta* **2009**, *54*, 7471-7475.
[55] G. Q. Liu, Y. J. Wang, Qilu, W. Li, Chenhui, *Electrochim Acta* **2005**, *50*, 1965-1968.
[56] Y. Y. Sun, Y. F. Yang, H. Zhan, H. X. Shao, Y. H. Zhou, *J Power Sources* **2010**, *195*, 4322-4326.
[57] M. Kunduraci, J. F. Al-Sharab, G. G. Amatucci, *Chem Mater* **2006**, *18*, 3585-3592.
[58] X. L. Zhang, F. Y. Cheng, K. Zhang, Y. L. Liang, S. Q. Yang, J. Liang, J. Chen, *Rsc Adv* **2012**, *2*, 5669-5675.
[59] G. B. Zhong, Y. Y. Wang, Z. C. Zhang, C. H. Chen, *Electrochim Acta* **2011**, *56*, 6554-6561.
[60] H. Y. Xu, S. Xie, N. Ding, B. L. Liu, Y. Shang, C. H. Chen, *Electrochim Acta* **2006**, *51*, 4352-4357.
[61] J. H. Kim, S. T. Myung, Y. K. Sun, *Electrochim Acta* **2004**, *49*, 219-227.
[62] X. K. Huang, Q. S. Zhang, J. L. Gan, H. T. Chang, Y. Yang, *J Electrochem Soc* **2011**, *158*, A139-A145.
[63] P. Strobel, A. I. Palos, M. Anne, F. Le Cras, *J Mater Chem* **2000**, *10*, 429-436.
[64] J. H. Kim, S. T. Myung, C. S. Yoon, S. G. Kang, Y. K. Sun, *Chem Mater* **2004**, *16*, 906-914.
[65] Y. Talyosef, B. Markovsky, G. Salitra, D. Aurbach, H. J. Kim, S. Choi, *J Power Sources* **2005**, *146*, 664-669.

Received: ((will be filled in by the editorial staff))
Published online: ((will be filled in by the editorial staff))